Synchronized renal tubular cell death involves ferroptosis

Andreas Linkermann[a,1], Rachid Skouta[b], Nina Himmerkus[c], Shrikant R. Mulay[d], Christin Dewitz[a], Federica De Zen[a], Agnes Prokai[e], Gabriele Zuchtriegel[f,g], Fritz Krombach[f,g], Patrick-Simon Welz[h,i], Ricardo Weinlich[j], Tom Vanden Berghe[k,l], Peter Vandenabeele[k,l], Manolis Pasparakis[i], Markus Bleich[c], Joel M. Weinberg[m], Christoph A. Reichel[f,g], Jan Hinrich Bräsen[n], Ulrich Kunzendorf[a], Hans-Joachim Anders[d], Brent R. Stockwell[o,p,q,r], Douglas R. Green[j], and Stefan Krautwald[a,1]

[a]Clinic for Nephrology and Hypertension, Christian-Albrechts-University Kiel, 24105 Kiel, Germany; [b]Department of Biological Sciences and Department of Chemistry, University of Texas at El Paso, El Paso, TX 79902; [c]Department of Physiology, Christian-Albrechts-University Kiel, 24098 Kiel, Germany; [d]Nephrologisches Zentrum, Medizinische Klinik und Poliklinik IV, Klinikum der Universität München, Ludwig-Maximilians-Universität München, 80366 Munich, Germany; [e]First Department of Pediatrics, Semmelweis University, H-1083 Budapest, Hungary; [f]Department of Otorhinolaryngology, Head and Neck Surgery, Ludwig-Maximilians-Universität München, 81366 Munich, Germany; [g]Walter Brendel Centre of Experimental Medicine, Ludwig-Maximilians-Universität München, 81366 Munich, Germany; [h]Institute for Research in Biomedicine, 08028 Barcelona, Spain; [i]Institute for Genetics, University of Cologne, 50931 Cologne, Germany; [j]Department of Immunology, St. Jude Children's Research Hospital, Memphis, TN 38105-3678; [k]Molecular Signaling and Cell Death Unit, Inflammation Research Center, Vlaams Instituut voor Biotechnologie, Ghent University, 9052 Ghent, Belgium; [l]Methusalem Program, Ghent University, 9052 Ghent, Belgium; [m]Division of Nephrology, Department of Internal Medicine, VA Healthcare System and University of Michigan, Ann Arbor, MI 48109-5676; [n]Department of Pathology, University of Hannover, 30625 Hannover, Germany; [o]Department of Biological Sciences, Columbia University, New York, NY 10027; [p]Department of Chemistry, Columbia University, New York, NY 10027; [q]Howard Hughes Medical Institute, Columbia University, New York, NY 10027; and [r]Department of Systems Biology, Columbia University Medical Center, New York, NY 10027

Edited* by Vishva M. Dixit, Genentech, San Francisco, CA, and approved October 10, 2014 (received for review August 12, 2014)

Receptor-interacting protein kinase 3 (RIPK3)-mediated necroptosis is thought to be the pathophysiologically predominant pathway that leads to regulated necrosis of parenchymal cells in ischemia–reperfusion injury (IRI), and loss of either Fas-associated protein with death domain (FADD) or caspase-8 is known to sensitize tissues to undergo spontaneous necroptosis. Here, we demonstrate that renal tubules do not undergo sensitization to necroptosis upon genetic ablation of either FADD or caspase-8 and that the RIPK1 inhibitor necrostatin-1 (Nec-1) does not protect freshly isolated tubules from hypoxic injury. In contrast, iron-dependent ferroptosis directly causes synchronized necrosis of renal tubules, as demonstrated by intravital microscopy in models of IRI and oxalate crystal-induced acute kidney injury. To suppress ferroptosis in vivo, we generated a novel third-generation ferrostatin (termed 16-86), which we demonstrate to be more stable, to metabolism and plasma, and more potent, compared with the first-in-class compound ferrostatin-1 (Fer-1). Even in conditions with extraordinarily severe IRI, 16-86 exerts strong protection to an extent which has not previously allowed survival in any murine setting. In addition, 16-86 further potentiates the strong protective effect on IRI mediated by combination therapy with necrostatins and compounds that inhibit mitochondrial permeability transition. Renal tubules thus represent a tissue that is not sensitized to necroptosis by loss of FADD or caspase-8. Finally, ferroptosis mediates postischemic and toxic renal necrosis, which may be therapeutically targeted by ferrostatins and by combination therapy.

regulated cell death | programmed cell death | ferroptosis | necroptosis | apoptosis

Regulated cell death may result from immunologically silent apoptosis or from immunogenic necrosis (1–3). Necroptosis, the best-characterized pathway of regulated necrosis, involves activation of receptor-interacting protein kinase 3 (RIPK3)-mediated phosphorylation of mixed lineage kinase domain-like protein (pMLKL) and subsequent plasma-membrane rupture, which was demonstrated in several disease states, including ischemia–reperfusion injury (IRI) in all organs analyzed (2–6); however, none of these previous studies clearly investigated the mode of cell death in the primary parenchymal cells. Therefore, it remained possible that the protective effects reported upon application of the necroptosis inhibitor necrostatin-1 (Nec-1) and for RIPK3-ko mice involve vascular, nonparenchymal effects. This possibility has been ruled out in non-IRI settings by conditional tissue targeting of proteins involved in the prevention of spontaneously occurring necroptosis, such as RIPK1, and components that regulate its ubiquitinylation status [linear ubiquitinylation chain assembly complex (LUBAC), cellular inhibitors of apoptosis proteins (cIAPs)), caspase-8, and Fas-associated protein with death domain (FADD)] in the gastrointestinal tract (7, 8), the skin (9, 10), the liver (11), and immune cells (12, 13), all of which result in spontaneous RIPK3-mediated tissue necroptosis and inflammation (7–9, 11, 12, 14–17).

Ferroptosis is an iron-dependent necrotic type of cell death that occurs due to lipid peroxide accumulation, which routinely is prevented by glutathione peroxidase 4 (GPX4), a glutathione-(GSH)-dependent enzyme, and therefore depends on the functionality of a glu/cys antiporter in the plasma membrane referred to as system X_c^--minus (18–20). Ferroptosis has been reported to cause several diseases and may be interfered with in vitro by the small molecule ferrostatin-1 (Fer-1) (18); however, Fer-1 was suggested to have low in vivo functionality due to potential metabolic and plasma instability.

Significance

Cell death by regulated necrosis causes tremendous tissue damage in a wide variety of diseases, including myocardial infarction, stroke, sepsis, and ischemia–reperfusion injury upon solid organ transplantation. Here, we demonstrate that an iron-dependent form of regulated necrosis, referred to as ferroptosis, mediates regulated necrosis and synchronized death of functional units in diverse organs upon ischemia and other stimuli, thereby triggering a detrimental immune response. We developed a novel third-generation inhibitor of ferroptosis that is the first compound in this class that is stable in plasma and liver microsomes and that demonstrates high efficacy when supplied alone or in combination therapy.

Author contributions: A.L., T.V.B., M.B., J.M.W., C.A.R., U.K., H.-J.A., B.R.S., D.R.G., and S.K. designed research; A.L., R.S., N.H., S.R.M., C.D., F.D.Z., A.P., G.Z., F.K., T.V.B., J.M.W., J.H.B., and S.K. performed research; A.L., R.S., P.-S.W., R.W., P.V., M.P., M.B., H.-J.A., B.R.S., D.R.G., and S.K. contributed new reagents/analytic tools; A.L., R.S., N.H., S.R.M., P.-S.W., R.W., T.V.B., P.V., M.B., J.M.W., C.A.R., J.H.B., U.K., H.-J.A., B.R.S., D.R.G., and S.K. analyzed data; and A.L. wrote the paper.

The authors declare no conflict of interest.

*This Direct Submission article had a prearranged editor.

[1]To whom correspondence may be addressed. Email: andreas.linkermann@uksh.de or krautwald@nephro.uni-kiel.de.

This article contains supporting information online at www.pnas.org/lookup/suppl/doi:10.1073/pnas.1415518111/-/DCSupplemental.

In the present studies, we used inducible, conditional kidney tubule-specific genetic deletion of FADD and caspase-8, intravital microscopy, fresh isolation of primary kidney tubules, and four preclinical models of acute organ failure to further assess the relative roles of necroptosis and ferroptosis. We find that ferroptosis is of functional in vivo relevance in acute tubular necrosis and IRI, and we introduce, to our knowledge, the first ferroptosis inhibitor that is applicable for inhibition of ferroptosis in vivo. We conclude that specific combinatory therapies will be most promising for the prevention of clinically relevant IRI and that the nephron represents, to our knowledge, the first described tissue that is not sensitized to necroptosis by loss of FADD or caspase-8.

Results

Conditional Deletion of FADD or Caspase-8 Does Not Induce Cell Death in Renal Tubular Epithelia. The mode of cell death of tubular cells in acute kidney injury (AKI) has been a matter of intense discussion (21, 22). Because RIPK3-deficient mice have been shown to be partially protected from IRI-induced tubular necrosis (4, 23) and because Nec-1 phenocopies this effect (21, 24, 25), it was hypothesized that necroptosis might be the mode of cell death that drives parenchymal cells into necrosis. However, it was not ruled out that tubular cell death might have occurred secondary to some changes outside the tubular compartment: e.g., in RIPK3-dependent organ perfusion, which might be altered also upon Nec-1 treatment if the necroptotic pathway was involved. In fact, a discrepancy between the strong in vivo protection and the marginal protective effect of RIPK3-deficient freshly isolated tubules would be consistent with this hypothesis (4). A powerful approach to definitively study the involvement of cell-specific necroptosis is to delete components of the necroptosis-suppressing complex, which consists of FADD, caspase-8, RIPK1, and FLIP (26, 27), and to analyze spontaneously occurring necroptosis. We therefore crossed tubular cell-specific inducible conditional mice (Pax8-rtTA Tet-on.Cre) (28) to FADD or capase-8 floxed mice (Fig. S1 *A*–*E*) and confirmed the deficiency of the protein of interest by Western blotting from freshly isolated renal tubules (Fig. 1 *A* and *B* and *D* and *E*), which were carefully confirmed to be devoid of any other cells (Fig. S2). Unlike in all other tissues reported so far, inducible deletion of FADD or caspase-8 in Pax8-rtTA; Tet-on.Cre × FADD fl/fl and Pax8-rtTA; Tet-on.Cre × caspase-8 fl/fl mice did not affect serum markers of renal function (Fig. 1*G* and Fig. S1*F*), histological appearance (Fig. 1 *C* and *F*), or organ function for the entire observation period of 3 wk after addition of doxycyclin into the drinking water (Fig. 1*G* and Fig. S1*F*). After the 3-wk period of doxycyclin feeding, mice were morphologically indistinguishable from nondoxy-fed littermates (Fig. S1*E*). In addition, induction of acute kidney injury by application of the nephrotoxin cisplatin (20 mg/kg body weight) led to similar survival kinetics as in WT mice (Fig. 1*H*). In freshly isolated renal tubules treated with 50 μM Nec-1, no protection was detected both in the presence or in the absence of glycine (Fig. 1*I*). This result is in line with our previous observation of low levels of RIPK3 in tubular cell lines (21) and marginal sensitivity for necroptosis compared with a glomerular endothelial cell line and L929 fibrosarcoma cells (21). Taken together, these data strongly argue against necroptosis as the primary mode of regulated cell death in renal tubules and suggest that the effects in RIPK3-ko and Nec-1–treated mice are due to extratubular effects.

RIPK3-Deficient Mice Exhibit Increased Renal Perfusion and Fail To Gain Normal Body Weight. Using low-resolution intravital microscopy, we previously investigated the effects of Nec-1 on the diameter of peritubular capillaries (22). Using a similar approach with higher resolution (Fig. S3*A*), we have now analyzed RIPK3-ko mice and detected statistically significant increases in peritubular diameters (Fig. S3 *B* and *C*), which would account for 25.7% increase in blood flow (Fig. S3*D*) according to the law of Hagen Poiseuille and could help maintain peritubular perfusion after ischemia when it is known to be compromised. Taking into consideration that, in all renal cells investigated, the highest RIPK3 expression was found in endothelial cells, vascular effects cannot be ruled out, and endothelial cell-specific conditional RIPK3 depletion should be investigated in IRI models. In this respect, it is noteworthy that, in another model of necrotic parenchymal damage that does not rely on ischemia–reperfusion

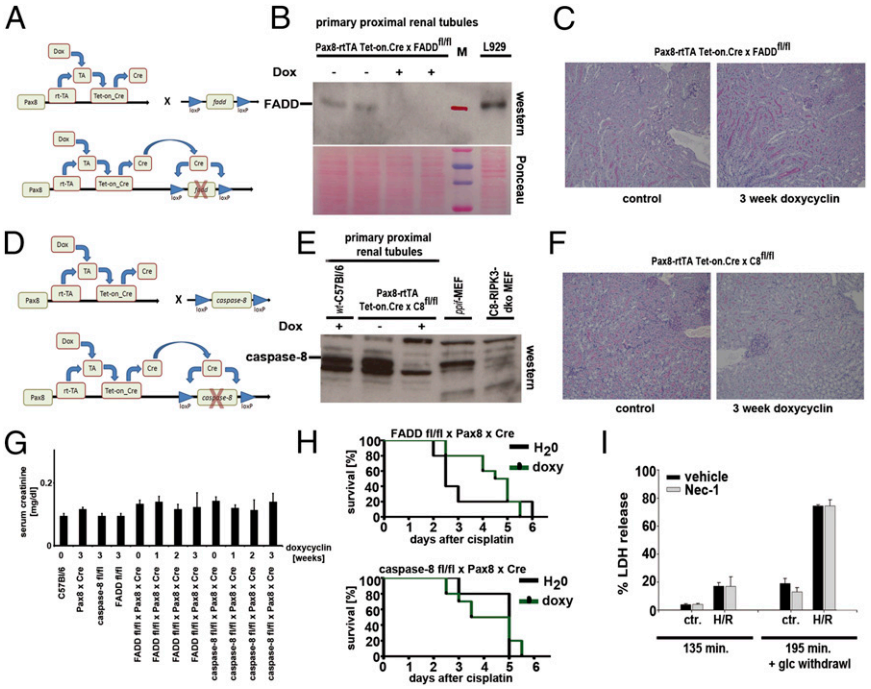

Fig. 1. Conditional deletion of FADD or caspase-8 does not sensitize renal tubules to necroptosis. (*A*) Scheme of the doxycyclin-inducible conditional tubular knockout. (*B*) After 3 wk of doxycyclin-treatment, no detection of the FADD protein in freshly isolated renal tubules was possible; L929 cells serve as a positive control. (*C*) Periodic acid–Schiff (PAS) staining of normal renal morphology in Pax8-rtA; Tet-on.Cre × FADD fl/fl mice after 3-wk treatment with doxycyclin via the drinking water. (*D*–*F*) Similarly, caspase-8 was inducibly depleted from tubules. Note that the anti-mouse monoclonal antibody against caspase-8 cross-reacts with a nonspecific protein just below the band of caspase-8. Mouse embryonic fibroblasts (MEFs) from caspase-8/RIPK3-dko mice serve as a negative control, MEFs from cyclophilin D-deficient *ppif*-ko mice serve as a positive control, as do the C57BL/6 WT mice. (*G*) Serum creatinine levels remain in the normal range in all mice investigated as indicated. (*H*) Doxycyclin-induced conditional FADD-deficient or caspase-8–deficient mice react to 20 mg/kg body weight cisplatin-induced acute kidney injury similarly to nonstimulated mice. (*I*) Necrostatin-1 (Nec-1; 50 μM) does not influence the amount of LDH released from hypoxic renal tubules, either in the presence (*Left*) or absence (*Right*) of glycine (glc) (n = 8–10 per group).

injury, the cerulein-induced pancreatitis, in our hands, RIPK3-deficient mice are not protected from the increase in serum levels of amylase and lipase (Fig. S3*E*). In addition, we noticed that RIPK3-ko mice fail to gain normal body weight in comparison with WT littermates in both males and females (Fig. S3 *F* and *G*).

Morphological Changes of Synchronized Tubular Cell Death Are Prevented by Ferrostatins. If apoptosis and necroptosis account for only minor damage of acute tubular necrosis, we asked what pathway of regulated necrosis might be causative of synchronized tubular death that we identified in an improved ex vivo model of freshly isolated murine renal tubules upon depletion of fatty acids (Fig. 2*A* and Movie S1). We confirmed such tubules to be functional before the onset of the fatty-acid depletion for maximal control purposes (Movie S2). Importantly, such synchronized tubular (cell) death very much resembles the appearance of casts found in urine sediments of patients with acute kidney injury. The dynamics of the tubular necrosis suggest a direct cell-to-cell communication to deliver the deadly signal (Movie S3). Because we previously reported a beneficial effect of the second-generation ferrostatin 11-92 (29) in a model of acute injury of freshly isolated renal tubules, we looked for the morphology of such tubules in the presence of erastin, a well-described inducer of ferroptosis, a necrotic type cell death that largely depends on lipid peroxidation (18, 19), over time (Fig. 2*B*). Whereas the

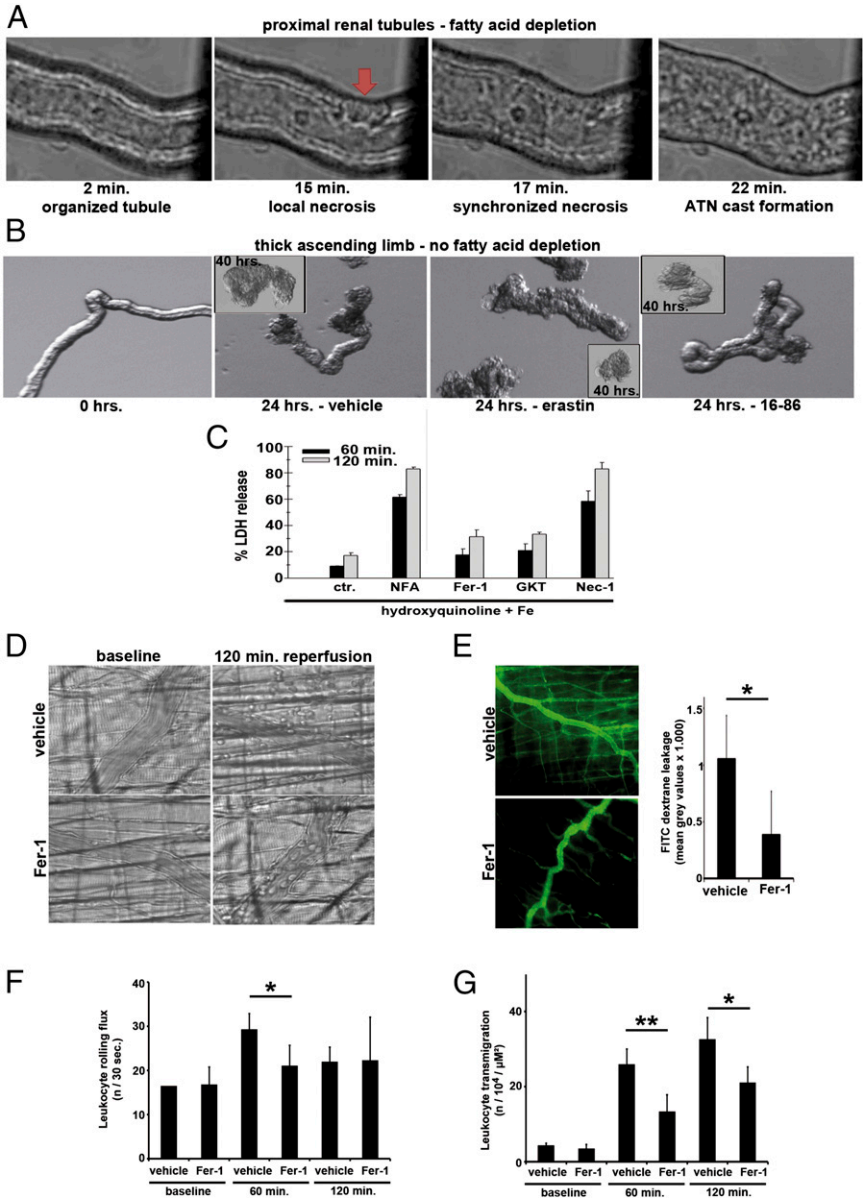

Fig. 2. Ferroptosis mediates synchronized tubular necrosis and contributes to immune-cell extravasation into ischemic tissue. (*A*) Snapshots from Movie S1 of functional freshly isolated proximal renal tubule segments undergoing rapid synchronized necrosis upon fatty-acid depletion. (*B*) In the presence of fatty acids, addition of erastin accelerated, whereas 16–86 (a third-generation ferrostatin; see Fig. 3) prevented, tubular necrosis. (*C*) During the time course of hydroxyquinoline/Fe-induced tubular necrosis, Fer-1 and the Nox-inhibitor GKT prevented LDH release whereas Nec-1 did not show protection. (*D*) Reflected light oblique transillumination imaging of leukocyte passages through postcapillary venules in IRI of the cremaster muscle in the presence of vehicle or Fer-1. (*E*) FITC dextran leakage in the same model. (*F*) Leukocyte rolling is affected by Fer-1 within the first hour after reperfusion. (*G*) Significantly reduced leukocyte transmigration in the presence of Fer-1.

faint plasma membrane of untreated tubules did not change in 16-86–treated tubules [a novel third-generation ferrostatin we generated (Fig. 3)], vehicle-treated and especially erastin-treated tubules showed membrane protrusions and obvious signs of deformation and functional insufficiency (Fig. 2*B*). When erastin was applied into the tubule, a similar type of cell death occurred even without fatty-acid depletion (Movie S4). In another well-established lactate dehydrogenase (LDH) release-based assay of ex vivo tubulotoxicity (29), hydroxyquinoline–iron-induced cell death, we found Fer-1 and the Nox-inhibitor GKT to be protective whereas Nec-1 did not show any protection (Fig. 2*C*).

Ferroptosis Mediates IRI-Mediated Immune-Cell Infiltration of the Cremaster Muscle. The concept of immunogenic necrotic cell death proposes to trigger an autoamplification loop, which is triggered by a necroinflammatory microenvironment. To understand how ferroptosis attracts immune cells during hypoxia/reperfusion situations, we performed musculus cremaster IRI assays and read out the immune-cell infiltration by intravital microscopy (Fig. 2 *D–F*) and quantified rolling, adherent, and transmigrated cells in the presence and absence of ferrostatins (Fig. 2 *F* and *G* and Fig. S4 *A* and *B*). Less immune-cell infiltration into the postischemic area suggested either that Fer-1 directly inhibits leukocyte transmigration or that the local proinflammatory microenvironment was less chemoattractive, presumably by less damage-associated molecular pattern (DAMP) release due to less ferroptotic cell death.

Ferroptosis Mediates Tubule Necrosis in Oxalate Nephropathy, but Not in an LPS-Induced Septic Shock Model. Having identified ferroptosis to be of relevance in acute postischemic injury, we sought to investigate another model of acute renal failure, oxalate nephropathy, which has recently been established (30). Intrarenal CaOx crystal deposition was identical in all groups (Fig. S5 *A* and *B*). However, neutrophil infiltration and expression levels of proinflammatory cytokines (CXCL-2, IL-6), kidney injury molecule 1 (KIM-1), and the p65 subunit of NF-κB were statistically significantly reduced upon a once daily i.p. application of Fer-1 (Fig. S5*E*). Importantly, Fer-1 also significantly reduced the tubular injury score (Fig. S5*D*) and the functional serum markers of kidney injury creatinine and urea (Fig. S5*C*). Because RIPK3-deficient mice have been demonstrated to be resistant to sepsis models, we also investigated Fer-1 in the model of LPS-induced shock (Fig. S5*F*), but no difference compared with vehicle-treated mice was evident. Therefore, ferroptosis seems to be a valuable target for both postischemic and toxic acute kidney injury. However, given the poor plasma stability of Fer-1, we sought to develop a more stable compound for the in vivo applications.

Generation of a Third-Generation Ferrostatin with Increased Plasma and Metabolic Stability for in Vivo Studies. Given the promising results of the cremaster–IRI and oxalate nephropathy studies and the previously published efficacy of second-generation ferrostatins in models of Huntington´s disease, periventricular leukomalacia, and tubular necrosis (29), we wondered whether the reported poor plasma stability of Fer-1 could be further enhanced by structure-relation analysis. We therefore first evaluated the in vitro metabolic stability of one of the highly potent Fer-1 analogs, SRS15-72B (29), in liver microsomes of mice. SRS15-72B was cleared rapidly with a half-life of $t_{1/2} = 2$ min (Table S1). To achieve a more metabolically stable Fer-1 analog, we created an imine-type structure (SRS15-72A) that showed high stability in microsomes with a half-life of $t_{1/2} = 154$ min (Table S2). This metabolically stable analog turned out not to be sufficiently stable in the plasma due to its ethyl ester moiety (Table S3), a functional group well-known to be more susceptible to hydrolysis in plasma (31). Because a previous study showed that the ethyl ester is important to maintain the potency of Fer-1, we aimed at improving the plasma stability, while maintaining high microsomal stability by creating additional imine analogs with isopropyl (SRS16-80) and *tert*-butyl (SRS16-86) esters (Fig. 3*A*). These analogs allowed us to comparatively study the plasma stability of the ethyl, isopropyl, and *tert*-butyl esters, respectively. Among these three ester analogs (SRS15-72A, SRS16-80, and SRS16-86), the *tert*-butyl ester analog (SRS16-86) showed the highest stability in plasma (Table S4). In addition, SRS16-86 maintains high stability in the microsomal compartment [intrinsic clearance (CLint) (mL/min per g liver < 0.5)] (Table S5). For in vivo experiments, we therefore used 16-86 and used it in comparison with 16–79, an inactive derivate (Fig. 3*B*). We confirmed the ferroptosis-inhibiting ability of 16-86 and 16-79 in vitro by FACS analysis of erastin-treated HT-1080 cells and in NIH 3T3 cells (Fig. 3*C*). In both necroptosis and ferroptosis, we failed to detect cleaved caspase 3 (Fig. 3*D*).

Ferroptosis Mediates Necrotic Tubular Cell Death in Renal Ischemia–Reperfusion Injury. We applied active (16-86) and inactive (16-79) compounds to a model of severe ischemia–reperfusion injury (IRI), which we described before (4). Upon 40 min of ischemia before reperfusion, we know that all WT mice die between 48 h and 72 h, which can be anticipated from the 48-h serum creatinine values above 2.0 mg/dL. As demonstrated in Fig. 4 *A–D*, creatinine levels of all vehicle-treated C57BL/6 mice exceeded 2.0 mg/dL and showed strong morphologic damage and high serum urea levels whereas Fer-1–treated and, to a greater extent,

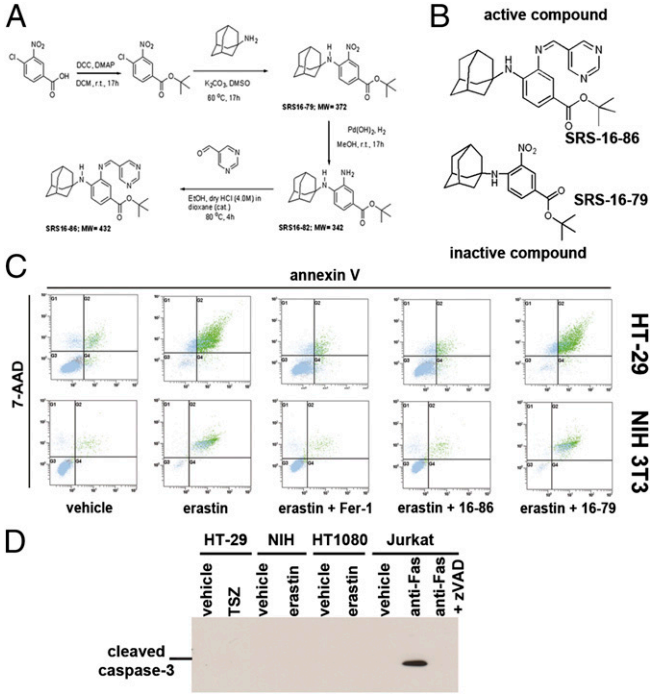

Fig. 3. Generation and in vitro testing of a ferrostatin derivative for in vivo applications. (*A*) Synthetic route of the most microsomal and plasma stable ferrostatin analog (SRS16-86). (*B*) Model structure of the two novel ferrostatin derivates SRS16-79 (inactive compound) and SRS16-86 (active compound). (*C*) FACS analysis for the necrotic marker 7AAD and phosphatidylserine accessibility (annexin V) in HT1080 and NIH 3T3 cells treated with either vehicle or 50 μM erastin in the presence or absence of 1 μM Fer-1, 16-86, or 16-79. (*D*) Absence of cleaved caspase-3 in necroptosis and ferroptosis. Western blot of cleaved caspase-3 in lysates from 100 ng/mL TNFα plus 1 μM Smac mimetics plus 25 μM zVAD-treated HT-29 cells, 50 μM erastin-treated NIH 3T3 cells, and 50 μM erastin-treated HT1080 cells for 24 h. Monoclonal anti-Fas–treated Jurkat cells (100 ng/mL) served as positive control. TSZ, TNFa/SMAC-mimetic/zVAD.

16-86–treated mice were protected from functional acute renal failure (Fig. 4 *C* and *D*) and structural organ damage (Fig. 4 *A* and *B*) after IRI. Mice treated with 16–79 in a similar manner did not show any differences compared with the vehicle-treated controls. We did not observe any side effects from treatment with the same dose of 16-86 4 wk after application. The effect of 16-86 exceeded that of any single compound we previously experienced to be protective from renal IRI.

Ferrostatins Further Increase the Protective Effect of [Necrostatin-1/Sanglifehrin A] Combination Therapy in Renal IRI. Given that Nec-1 protects from renal IRI to a lesser extent than 16-86, and given that interference with mitochondrial permeability transition (MPT)-induced regulated necrosis (MPT-RN) by the compound sanglifehrin A (SfA) also mildly protects from IRI, with marked additive protective effects in combination therapy with Nec-1 (4, 5), we sought to further extend the combination therapy by investigating the influence of 16-86 and 16-79 in [Nec-1 + SfA]-treated mice. Because the effect of the [Nec-1 + SfA] treatment could be investigated only in a severe ischemia model and we aimed to investigate additive protective effects by 16-86, we further increased the ischemic duration to a model of ultrasevere IRI (see *Materials and Methods* for details). In such settings, even the combination therapy with [Nec-1 + SfA] did not fully rescue creatinine values and organ damage (Fig. 4 *E–H*). Addition of 16-86, but not 16-79, reduced plasma levels of serum urea and serum creatinine, suggesting that a triple combination therapy with [Nec-1 + SfA] plus 16-86 is superior in the prevention of renal IRI compared with the double-combination therapy with [Nec-1 + SfA]. In addition, this result indicates either that at least three independent pathways of regulated necrosis may be involved in IR-mediated organ damage or that inhibition of overlapping elements with SfA and Nec-1 are incomplete.

Discussion

Parenchymal cell necrosis, but not apoptosis, which seems to be minimally involved in the pathogenesis of acute kidney injury (32), triggers the release of DAMPs, some of which can trigger regulated necrosis and therefore initiate a necroinflammatory feedback loop. In clinical routine, immunosuppression is a standard procedure, but an anti-cell death therapy does not exist apart from cyclosporine (5). Therefore, defining the precise mechanisms that trigger regulated necrosis is essential for the development of new drugs. Our data indicate that alternative interpretations apart from "pure" necroptosis exist and suggest that ferroptosis is of importance in renal tubules, which, other than the skin, the gastrointestinal tract, or immune cells, do not depend on a necroptosis-inhibiting complex, at least not of FADD and caspase-8. To date, it cannot be ruled out that previously described protection against ischemia–reperfusion injury in diverse organs is mediated by increased perfusion rather than direct protection from parenchymal necroptosis. Our results regarding the cerulein-induced pancreatitis are in line with this

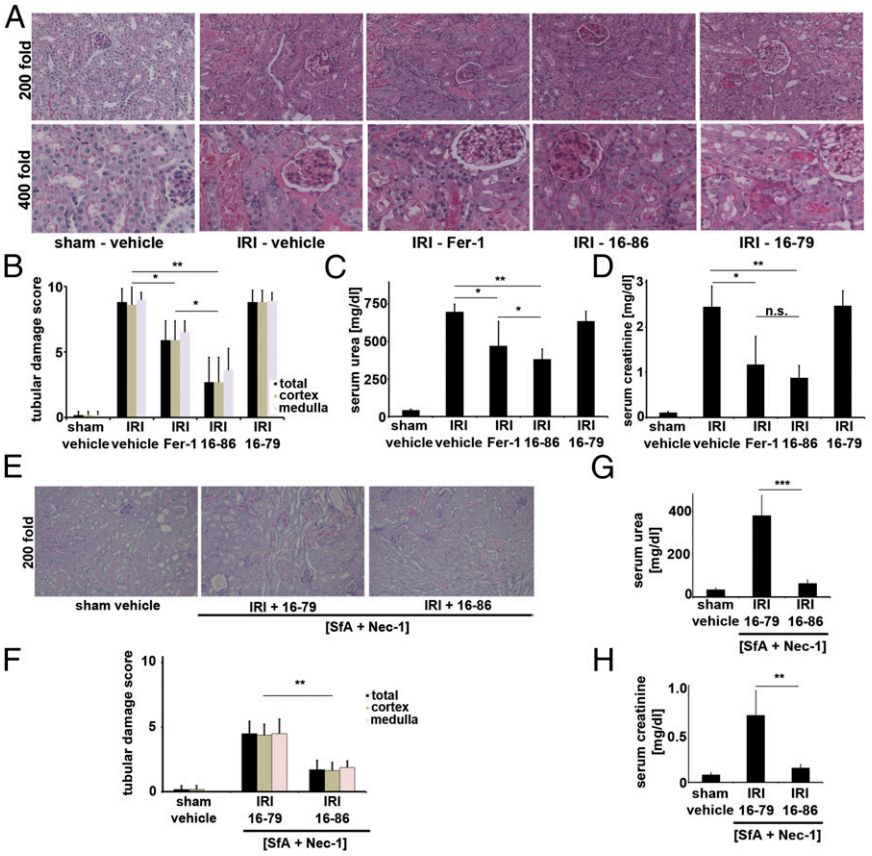

Fig. 4. Ferroptosis significantly contributes to renal ischemia–reperfusion injury. (*A* and *B*) Representative PAS stainings and quantification of renal damage from mice treated with severe ischemic durations before reperfusion. Mice were killed 48 h after reperfusion. (*C* and *D*) Functional markers of acute kidney injury after severe IRI (as in *A* and *B*). (*E* and *F*) Histologic PAS staining and quantification of sham operation or ultrasevere IRI (50 min of ischemia before reperfusion) in WT mice treated with [Nec-1 + SfA] combination therapy together with either 16-79 or 16-86. (*G* and *H*) C57BL/6 were treated as in *E*, and functional markers of acute kidney injury were measured 48 h after the onset of reperfusion. n.s., not significant; $*P = 0.05–0.02$, $**P = 0.02–0.001$, $***P \leq 0.001$; $n = 10$ per group in all experiments).

hypothesis and are in contrast to previously published data (33, 34). Several unanswered questions remain: Why are RIPK3-deficient mice protected in several models of IRI if the parenchymal cells do not undergo necroptosis? Why do necrostatins protect such tissues from organ failure if necroptosis is not the predominant mechanism of parenchymal cell death? Endothelial cell-specific deletion of RIPK3 will help to answer these open questions.

Materials and Methods

See *SI Materials and Methods* for detailed descriptions.

Mice. All WT mice reported in this study were on C57BL/6 background. Eight- to 12-wk-old male C57BL/6 mice (average weight ~23 g) were used for all WT experiments, unless otherwise specified. Caspase-8 fl/fl mice were kindly provided by Razquella Hakem (Department of Medical Biophysics, University of Toronto, Toronto and Ontario Cancer Institute, University Health Network, Toronto). FADD fl/fl mice were generated by and provided by M.P. Doxycyclin-inducible renal tubule-specific Pax8-rtTA; Tet-on.Cre mice have been published (28) and were kindly provided by Tobias B. Huber (Renal Division, University Medical Center Freiburg, Freiburg, Germany). RIPK3-deficient mice were kindly provided by Vishva M. Dixit (Genentech, San Francisco, CA). All in vivo experiments were performed according to the Protection of Animals Act, after approval of the German local authorities or the Institutional Animal Care and Use Committee (IACUC) of the University of Michigan, and the National Institutes of Health *Guide for the Care and Use of Laboratory Animals* (35), after approval from the University of Michigan IACUC or by the local authorities responsible for the approval at Ghent University. In all experiments, mice were carefully matched for age, sex, weight, and genetic background.

Histology, Immunohistochemistry, and Evaluation of Structural Organ Damage. Organs were dissected as indicated in each experiment and infused with 4% (vol/vol) neutral-buffered formaldehyde, fixated for 48 h, dehydrated in a graded ethanol series and xylene, and finally embedded in paraffin. Stained sections were analyzed using an Axio Imager microscope (Zeiss). Kidney damage was quantified by two experienced pathologists in a double-blind manner on a scale ranging from 0 (unaffected tissue) to 10 (severe organ damage). The following parameters were chosen as indicative of morphological damage to the kidney after ischemia–reperfusion injury (IRI): brush border loss, red blood cell extravasation, tubule dilatation, tubule degeneration, tubule necrosis, and tubular cast formation. These parameters were evaluated on a scale of 0–10, which ranged from not present (0), mild (1–4), moderate (5 or 6), severe (7 or 8), to very severe (9 or 10). Each parameter was determined on at least four different animals.

Statistics. For all experiments, differences of datasets were considered statistically significant when P values were lower than 0.05, if not otherwise specified. Statistical comparisons were performed using the two-tailed Student t test. Asterisks are used in the figures to specify statistical significance ($*P < 0.05$; $**P < 0.02$; $***P < 0.001$). P values in survival experiments (Kaplan–Meier plots) were calculated using GraphPad Prism, ver. 5.04 software. Statistics are indicated as SD unless otherwise specified.

ACKNOWLEDGMENTS. We thank Katja Bruch, Maike Berger, Janina Kahl, and Monika Iversen for excellent technical assistance and Justus Cordt for expert help with mouse weight charts. A.L. received funding from the German Society for Nephrology, the Else Kröner-Fresenius Stiftung, Pfizer, and Novartis. H.-J.A. is supported by Deutsche Forschungsgemeinschaft Grants AN372/9-2, AN371/12-2, and AN372/15-1 and the Else Kröner-Fresenius Stiftung. B.R.S. is an Early Career Scientist of the Howard Hughes Medical Institute and received funding from New York State Stem Cell Science (Contract C026715 for the Chemical Probe Synthesis Facility), the US National Institutes of Health (NIH Grants R01CA097061, R01GM085081, and R01CA161061), the Whitehall Foundation, the William Randolph Hearst Foundation, and the Baby Alex Foundation. J.M.W. is supported by NIH Grant R01DK34275 and the Veterans Administration. Research in the P.V. unit is supported by Belgian grants (Interuniversity Attraction Poles Grants IAP 6/18 and IAP 7/32), Flemish grants (Research Foundation Flanders Grants FWO G.0875.11, FWO G.0973.11 N, FWO G.0A45.12 N, FWO G.0172.12, FWO G.0787.13N, G0C3114N, and FWO KAN 31528711), Ghent University grants (Multidisciplinary Research Partnership, Ghent Researchers On Unfolded Proteins in Inflammatory Disease consortium), and grants from the Flanders Institute for Biotechnology. P.V. holds Methusalem Grant BOF09/01M00709 from the Flemish Government. S.K. received grants from Pfizer, Novartis, Fresenius, and the Else Kröner-Fresenius Stiftung.

1. Galluzzi L, Kepp O, Krautwald S, Kroemer G, Linkermann A (2014) Molecular mechanisms of regulated necrosis. *Semin Cell Dev Biol* 35C:24–32.
2. Kaczmarek A, Vandenabeele P, Krysko DV (2013) Necroptosis: The release of damage-associated molecular patterns and its physiological relevance. *Immunity* 38(2): 209–223.
3. Vanden Berghe T, Linkermann A, Jouan-Lanhouet S, Walczak H, Vandenabeele P (2014) Regulated necrosis: The expanding network of non-apoptotic cell death pathways. *Nat Rev Mol Cell Biol* 15(2):135–147.
4. Linkermann A, et al. (2013) Two independent pathways of regulated necrosis mediate ischemia-reperfusion injury. *Proc Natl Acad Sci USA* 110(29):12024–12029.
5. Linkermann A, Green DR (2014) Necroptosis. *N Engl J Med* 370(5):455–465.
6. Linkermann A, et al. (2013) Necroptosis in immunity and ischemia-reperfusion injury. *Am J Transplant* 13(11):2797–2804.
7. Günther C, et al. (2011) Caspase-8 regulates TNF-α-induced epithelial necroptosis and terminal ileitis. *Nature* 477(7364):335–339.
8. Welz PS, et al. (2011) FADD prevents RIP3-mediated epithelial cell necrosis and chronic intestinal inflammation. *Nature* 477(7364):330–334.
9. Bonnet MC, et al. (2011) The adaptor protein FADD protects epidermal keratinocytes from necroptosis in vivo and prevents skin inflammation. *Immunity* 35(4):572–582.
10. Gerlach B, et al. (2011) Linear ubiquitination prevents inflammation and regulates immune signalling. *Nature* 471(7340):591–596.
11. Liedtke C, et al. (2011) Loss of caspase-8 protects mice against inflammation-related hepatocarcinogenesis but induces non-apoptotic liver injury. *Gastroenterology* 141(6):2176–2187.
12. Osborn SL, et al. (2010) Fas-associated death domain (FADD) is a negative regulator of T-cell receptor-mediated necroptosis. *Proc Natl Acad Sci USA* 107(29):13034–13039.
13. Wong WW, et al. (2014) cIAPs and XIAP regulate myelopoiesis through cytokine production in an RIPK1- and RIPK3-dependent manner. *Blood* 123(16):2562–2572.
14. Ch'en IL, et al. (2008) Antigen-mediated T cell expansion regulated by parallel pathways of death. *Proc Natl Acad Sci USA* 105(45):17463–17468.
15. Kaiser WJ, et al. (2011) RIP3 mediates the embryonic lethality of caspase-8-deficient mice. *Nature* 471(7338):368–372.
16. Oberst A, et al. (2011) Catalytic activity of the caspase-8-FLIP(L) complex inhibits RIPK3-dependent necrosis. *Nature* 471(7338):363–367.
17. Zhang H, et al. (2011) Functional complementation between FADD and RIP1 in embryos and lymphocytes. *Nature* 471(7338):373–376.
18. Dixon SJ, et al. (2012) Ferroptosis: An iron-dependent form of nonapoptotic cell death. *Cell* 149(5):1060–1072.
19. Yagoda N, et al. (2007) RAS-RAF-MEK-dependent oxidative cell death involving voltage-dependent anion channels. *Nature* 447(7146):864–868.
20. Yang WS, et al. (2014) Regulation of ferroptotic cancer cell death by GPX4. *Cell* 156(1-2):317–331.
21. Linkermann A, et al. (2012) Rip1 (receptor-interacting protein kinase 1) mediates necroptosis and contributes to renal ischemia/reperfusion injury. *Kidney Int* 81(8):751–761.
22. Linkermann A, et al. (2013) The RIP1-kinase inhibitor necrostatin-1 prevents osmotic nephrosis and contrast-induced AKI in mice. *J Am Soc Nephrol* 24(10):1545–1557.
23. Luedde M, et al. (2014) RIP3, a kinase promoting necroptotic cell death, mediates adverse remodelling after myocardial infarction. *Cardiovasc Res* 103(2):206–216.
24. Degterev A, et al. (2005) Chemical inhibitor of nonapoptotic cell death with therapeutic potential for ischemic brain injury. *Nat Chem Biol* 1(2):112–119.
25. Smith CC, et al. (2007) Necrostatin: A potentially novel cardioprotective agent? *Cardiovasc Drugs Ther* 21(4):227–233.
26. Dillon CP, et al. (2012) Survival function of the FADD-CASPASE-8-cFLIP(L) complex. *Cell Reports* 1(5):401–407.
27. Dillon CP, et al. (2014) RIPK1 blocks early postnatal lethality mediated by caspase-8 and RIPK3. *Cell* 157(5):1189–1202.
28. Traykova-Brauch M, et al. (2008) An efficient and versatile system for acute and chronic modulation of renal tubular function in transgenic mice. *Nat Med* 14(9): 979–984.
29. Skouta R, et al. (2014) Ferrostatins inhibit oxidative lipid damage and cell death in diverse disease models. *J Am Chem Soc* 136(12):4551–4556.
30. Mulay SR, et al. (2013) Calcium oxalate crystals induce renal inflammation by NLRP3-mediated IL-1β secretion. *J Clin Invest* 123(1):236–246.
31. Di L, Kerns EH, Hong Y, Chen H (2005) Development and application of high throughput plasma stability assay for drug discovery. *Int J Pharm* 297(1-2):110–119.
32. Linkermann A, et al. (2014) Regulated Cell Death in AKI. *J Am Soc Nephrol*, ASN.2014030262.
33. He S, et al. (2009) Receptor interacting protein kinase-3 determines cellular necrotic response to TNF-alpha. *Cell* 137(6):1100–1111.
34. Zhang DW, et al. (2009) RIP3, an energy metabolism regulator that switches TNF-induced cell death from apoptosis to necrosis. *Science* 325(5938):332–336.
35. National Research Council (2011) *Guide for the Care and Use of Laboratory Animals* (National Academies Press, Washington, DC), 8th Ed.